Int. J. Environ. Res., 4(4):741-750 , Autumn 2010
ISSN: 1735-6865

Efficiency of Landsat ETM+ Thermal Band for Land Cover Classification of the Biosphere Reserve *"Eastern Carpathians"* (Central Europe) Using SMAP and ML Algorithms

Ehsani, A. H.[1*] and Quiel, F.[2]

[1]International Research Center for Living with Desert, University of Tehran, P.O. Box 14185-354 Tehran, Iran

[2]Department of Civil and Architectural Engineering, Royal Institute of Technology (KTH), SE-100 44 Stockholm, Sweden

Received 2 June 2009; Revised 10 March 2010; Accepted 25 July 2010

ABSTRACT: Two different methods of Bayesian segmentation algorithm were used with different band combinations. Sequential Maximum a Posteriori (SMAP) is a Bayesian image segmentation algorithm which unlike the traditional Maximum likelihood (ML) classification attempts to improve accuracy by taking contextual information into account, rather than classifying pixels separately. Landsat 7 ETM+ data with Path/Row 186-26, dated 30 September 2000 for a mountainous terrain at the Polish - Ukrainian border is acquired. In order to study the role of thermal band with these methods, two data sets with and without the thermal band were used. Nine band combinations including ETM+ and Principal Component (PC) data were selected based on the highest value of Optimum Index Factor (OIF). Using visual and digital analysis, field observation data and auxiliary map data like CORINE land cover, 14 land cover classes are identified. Spectral signatures were derived for every land cover. Spectral signatures as well as feature space analysis were used for detailed analysis of efficiency of the reflective and thermal bands. The result shows that SMAP as the superior method can improve Kappa values compared with ML algorithm for all band combinations with on average 17%. Using all 7 bands both SMAP and ML classifications algorithm achieved the highest Kappa accuracy of 80.37 % and 64.36 % respectively. Eliminating the thermal band decreased the Kappa values by about 8% for both algorithms. The band combination including PC1, 2, 3, and 4 (PCA calculated for all 7 bands) produced the same Kappa as bands 3, 4, 5 and 6. The Kappa value for band combination 3, 4, 5 and 6 was also about 4% higher than using 6 bands without the thermal band for both algorithms. Contextual classification algorithm like SMAP can significantly improve classification results. The thermal band bears complementary information to other spectral bands and despite the lower spatial resolution improves classification accuracy.

Key words: SMAP, Landsat ETM+, Thermal band, Maximum likelihood

INTRODUCTION

In the recent years various remote sensing techniques as well as geographical positioning systems have been widely used (Alesheikh *et al.*, 2007; Shobeiri *et al.*, 2007; Cetin, 2009; Solaimani, *et al.*, 2009; Pijanowski *et al.*, 2009). Wide area coverage, timely delivery, digital storage, low cost, repeatedly information acquisition also in areas with limited accessibility is of the advantages of remote sensing. Land cover, i.e. the composition and characteristics of land surface elements is a key information for many scientific and policy purposes and for sustainable management activities (Borak & Strahler, 1999; Chintan *et al.*, 2004; Cihlar, 2001; Ouattara *et al.*, 2004). Although land cove mapping is one of the earliest applications of remote sensing but the effect of a thermal band on classification accuracy and differentiation of land cover types still is not fully explored. The thermal band Landsat 7, ETM+6 is measuring the reflected solar radiation of electromagnetic radiation from 10.40 to 12.50 µm. Thermal sensors essentially measure the surface temperature and emitted radiation of targets but reflective bands measures the spectral reflectance of the surface at different wavelengths. Thus, TIR remote sensing data can significantly contribute to the observation, measurement, and analysis of energy balance characteristics (i.e., the fluxes and redistribution of thermal energy within and across the land surface) as an implicit and important aspect of landscape dynamics and landscape functioning (Dale

*Corresponding author E-mail:ehsani@ut.ac.ir

& Jeffrey 1999). Thermal information is complementary to visible and reflected infrared bands for the identification of different land covers. For instance Dator et al. (1998) demonstrate the best way to differentiate between gypsiferous and saline soils is to use the thermal band of Landsat TM in the classification. Their result showed that using the TM thermal band, the gypsiferous soils can be mapped in a relatively fast and accurate way (Dator et al., 1998). Alavi panah et al. (2007) used remote sensing to study soil salinity in the Ardakan area, Iran. They concluded that the behavior of TM thermal and reflective TM bands is highly depended on the type of land cover. In another study they also showed that thermal band is unique in identification of surface materials and features such as Yardangs in Lut desert (Alavi Panah et al., 2007). Since the source of thermal remote sensing is emitted energy from earth's surface, the handling and processing of thermal band is totally different from reflective bands. The different processing steps depend on the application of thermal band. Using thermal and reflective information together in classification algorithms such as Maximum likelihood (ML) and Sequential Maximum a Posteriori (SMAP) to increase land cover classification accuracy is one of the aims of this study. The other objective of this study is comparing the accuracy of a contextual classifiers like Sequential Maximum a Posteriori (SMAP) with a traditional Maximum likelihood (ML) algorithm. Per-pixel ML classification is limited by only utilizing spectral information without considering texture and contextual information (Dean & Smith, 2003; Gao et al., 2006; Pizzolato & Haertel, 2003; Zhou & Robson, 2001). Zhou and Robson (Zhou & Robson, 2001) claimed that texture information is ultimately necessary to obtain accurate image classification. Bouman and Shapiro (Bouman & Shapiro, 1994) also showed that with SMAP higher classification accuracy is achieved with ML for SPOT images. McCauley and Engel (McCauley *et al.*, 1977) compared two spectral/spatial scene segmentation algorithms (SMAP and ECHO, Extraction and Classification of homogenous Objects,) with ML. They found SMAP was better than ECHO and ML in all mean classification accuracies (McCauley et al., 1977). In this study increasing the Kappa accuracy by combining the thermal and reflective information using contextual classifiers is the main purpose.

The study area is centered on the common border point of Poland, Slovakia and Ukraine is located between 48° 52' N and 49° 25' N latitude, 21° 59' E and 23° 1' E longitude with a total area about 4543 Km^2 (Fig. 1). It covers the biosphere reserve "Eastern Carpathians" with the Bieszczady national park in Poland, Uzanski national park in Ukraine and Poloniny national park in Slovakia. Climatic conditions, different political and socioeconomic systems as well as ecological conditions resulted in complex landscape units. Land covers include deciduous forest dominated by beech (Fagus sylvatica) and sycamore (Acer Pseudoplatanus) in the central part, mixed forest dominated by beech and fir (Abies Alba) in the center and north eastern part, coniferous forest composed of fir, Norway spruce (Picea abies) and Scots pin (pinus Sylvestris) in Slovakia and Ukraine part (Kuemmerle *et al.*, 2006) . Grassland is the dominant landscape in the northwest, northeast and east. Arable lands are mostly found in the south west in Slovakia and in the north east in Ukraine.

MATERIALS & METHODS

The data set in this study consists of:

· Landsat ETM+ data path 186, row 26 dated 2000-09-30 (Fig.1) were acquired from the Global Land Cover Facility (GCLF) server at the University of Maryland, Institute for Advanced Computer Studies (UMIACS). GLCF provides free access to an integrated collection of critical land cover and earth science data (http://glcf.umiacs.umd.edu).

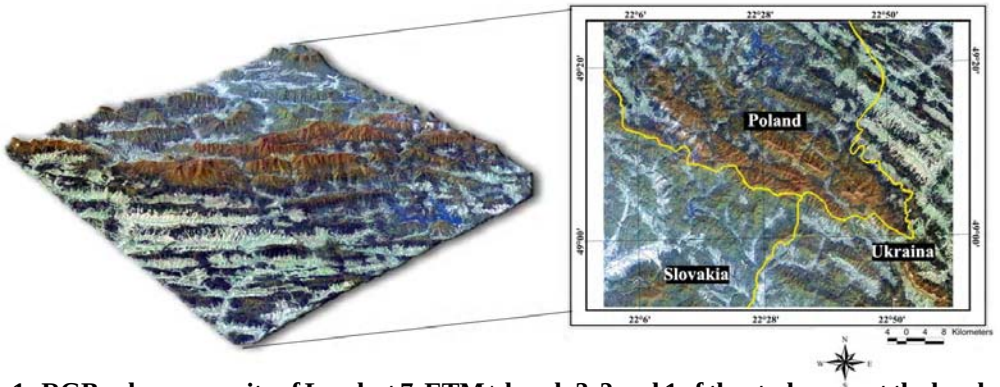

Fig. 1. RGB color composite of Landsat 7, ETM+ bands 3, 2 and 1 of the study area at the border of Poland, Slovakia and Ukraine.

· Auxiliary data such as a land cover map provided by Kuemmerle (Kuemmerle et al., 2006), topographic maps (scale 1:100 000) and field observation data.
· CORINE Land cover 2000 vector (http:// dataservice.eea.europa.eu)
· The 3 arc sec. digital elevation model derived from SRTM data (~90 m) was acquired from the National Aeronautics and Space Administrations (NASA) in geographic projection.

Open source GRASS (Geographic Resources Analysis Support System) Ver. 6.0, ENVI Ver.4.1 and ArcView Ver.3.2a softwares are used for image processing, classification and presentation of data.

Fig. 2 shows the overall methodology of this study. The ETM+ data were geo-referenced to UTM zone 34 with WGS 84 datum and then used for data processing.

Investigating correlation matrix between ETM+ bands may remarkably help to understand the bands correlation but obtaining a quantitative method for selecting the best bands combination is desirable. Chavez (Chavez, 1984) introduced Optimum Index Factor (OIF). The OIF method provides a measure of the spectral information content for optimum band selection in terms of band's variances and correlations. The OIF is calculated as Equation 1:

$$OIF = Std_i + Std_j + Std_k / |Corr\ i, j| + |Corr\ j, k| + |Corr\ i, k| \quad (1)$$

where: Std*i* : standard deviation of band I, Std*j*: standard deviation of band j, Std*k*: standard deviation of band k, Corr *ij*: correlation coefficient of band i and

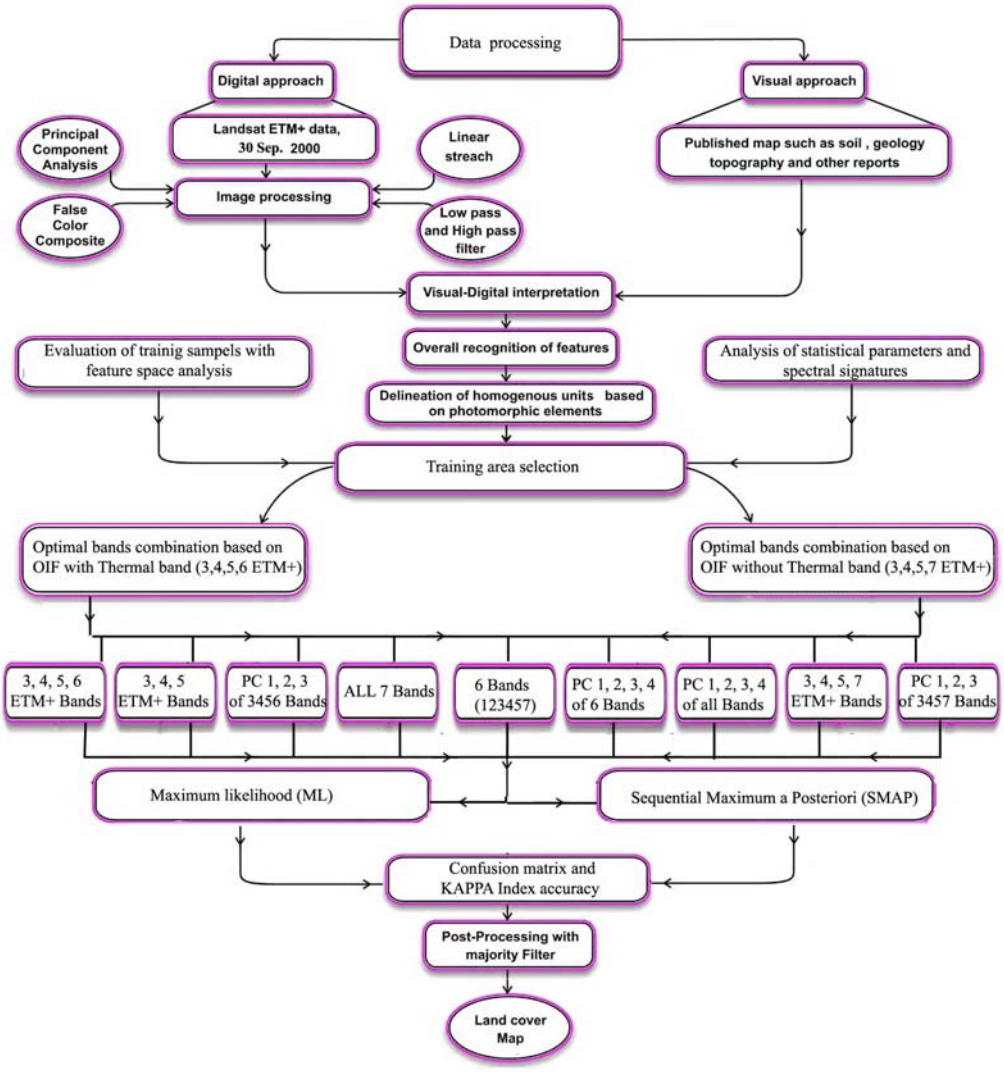

Fig. 2. Flowchart of the methodology

band j, Corr *ik*: correlation coefficient of band i and band k. Corr *jk*: correlation coefficient of band j and band k.

In this study two OIF sets, with and without thermal band in the data sets, were calculated. In order to achieve the objectives of this study, nine band combinations were selected. Bands with highest value of OIF calculation were included in three combinations of nine. Four band combinations also were selected from principal components analysis.

Two band combinations were including all seven ETM+ bands and six ETM+ bands excluding thermal band. All nine Band combinations were used as input for two different classifier algorithms. Contextual classifiers, Sequential Maximum a Posteriori (SMAP) and a traditional per-pixel Maximum likelihood (ML) algorithm were used. The ML, calculates (Bayesian) probability function from inputs for prototype vectors of each class. The data vectors consist of digital values from multi-spectral bands. Training samples are usually collected from field observations, aerial photos or previous land cover maps (Gao et al., 2006). This algorithm calculates the statistical probability based on the mean and covariance matrix of clusters. The probability membership value (L*i*(x)) of a pixel x to class *i* is:

$$L_i(X) = (2\delta)^{-n/2} |V_i|^{-1/2} e^{-y/2} \quad (2)$$

Where: V*i* is the covariance matrix of class *i*, n is the number of spectral bands and y is the Mahalanobis distance.

One limitation of ML algorithms is that each pixel is only assigned to one class and cause mixed pixel. Sequential Maximum a Posteriori (SMAP) attempts to improve classification accuracy by segmenting the image into regions rather than segmenting each pixel separately. This new procedure is proposed by Bouman and Shapiro (1994) and is calculated recursively. SMAP is a Bayesian image segmentation which uses the sequential maximum a posteriori estimator in conjunction with a novel multi scale random field (MSRF) and takes advantage of the spatial information of samples in the spectral bands. This kind of estimator minimizes the expected size of the largest misclassified region. The MSRF is composed of a sequence of random fields with coarse to fine scales. This method can be computed in time proportional to *MN* where *M* is the number of classes and *N* is the number of pixels. Details of the algorithm are given by Bouman and Shapiro (1994). Open source GRASS software version 6.0 (GRASS Development Team, 2006; Miliaresis & Paraschou, 2005) was used for both image classification algorithm. Co-occurrence image texture features (contrast, correlation, variance and entropy) were calculated for small sub regions of the classified image. Classification accuracies such as Kappa index, omission and commission error were calculated using confusion matrix analysis. Omission and commission error are related to producer's and user's accuracy respectively. The user accuracy is the probability that a certain reference class is classified as this class in the thematic map. The producer accuracy is the probability that a sample point in the map is that particular class. A standardized Z-test (Equation 3) incorporating the overall Kappa index and Kappa variance was used to determine if classifications were statistically significant different from one another (Congalton & Green, 1999).

$$Z = |k1-k2| / \text{sqrt}(var(k1) + var(k2)) \quad (3)$$

Where *k1* and *k2* are the two Kappa and var (*k1*) and var (*k2*) are their estimated variances. The hypothesis that two Kappas are equal is rejected for 95% confidence level if| Z | value is greater than 1.96. The| Z | value for confidence levels 90% and 85% are 1.64 and 1.44 respectively.

RESULTS & DISCUSSION

Feature space analysis was used to understand the relation between classes in two-dimensional spaces of ETM+ bands. Figure 3 shows the spatial distribution of different land cover classes between red (ETM+3) and near infrared (ETM+4) bands on the left (a) and ETM+4 and ETM+6 on the right (b). Characteristics of each land cover classes are shown in table 1. As it is obvious in fig3.a all land cover classes can be grouped into five major categories. Forest including deciduous with brownish leaves (class no. 6), mixed (class no. 8) and coniferous (class no.7) trees were easily separated from non- forest areas. Agricultural lands (class no.14) which at the time of image acquisition were harvested or plowed appear as a individual classes with low value in the infrared and red band. Fig3.b shows the land covers including to thermal properties. Harvested agricultural lands (class no.14) with bare soils absorb and re-emitting the higher percentage of the sun's energy and so have higher surface temperature than other classes such as forest or non- forested area. Forest area with green leaves due to evpotranspiration effects on temperature reduction shows a lower emitted energy than non-forest and agriculture area. Deciduous with brownish leave (class no.6) have the lowest radiant value in the study area.

Spectral signatures can be determined to identify individual land cover classes. By comparing the response patterns of different classes at different wavelengths we can distinguish between them. For example, water and vegetation may reflect similarly at visible

wavelengths but are almost always separable in the infrared. Spectral response can be quite variable, even for the same target type, and can also vary with time (e.g. "green-ness" of leaves) and location. Knowing where to "look" spectrally and understanding the factors which influence the spectral response of the features of interest are critical to correctly interpret the interaction of electromagnetic radiation with the surface. Figure 4 shows the spectral signature of two water classes. Red and near infrared radiation is absorbed more by water classes than shorter visible wavelengths. Class no. 12 includes the Solina reservoir in the Poland and Starina reservoir in the Slovakia but class no. 11 consist of streams, canals and rivers resulting in mixed pixels and higher values. Spectral signatures of four forest classes are shown in figure 5.

The internal structure of healthy leaves act as excellent reflectors of near-infrared wavelengths. So class no.13 (deciduous with green leaves) reflects more in all bands. Conversely, class no.7 (coniferous forest) which mainly covers the northeast of the study area has the lowest signature value in this group. Spectral signature of mixed forest (class no.8) is higher than for coniferous forest but lower than deciduous forest.

Figure 6 indicates the spectral signatures of the non-forest area. Class no.14 (agricultural lands) shows the different spectral response in all bands. This class tends to have reflection properties that increase approximately monotonically with wavelength. Due to factors such as the color, constituents and especially the moisture content, this class tends to have high reflectance in all bands. The class no.10 which is transitional zone between shrubs and forest shows the spectral signatures similar to these two groups.

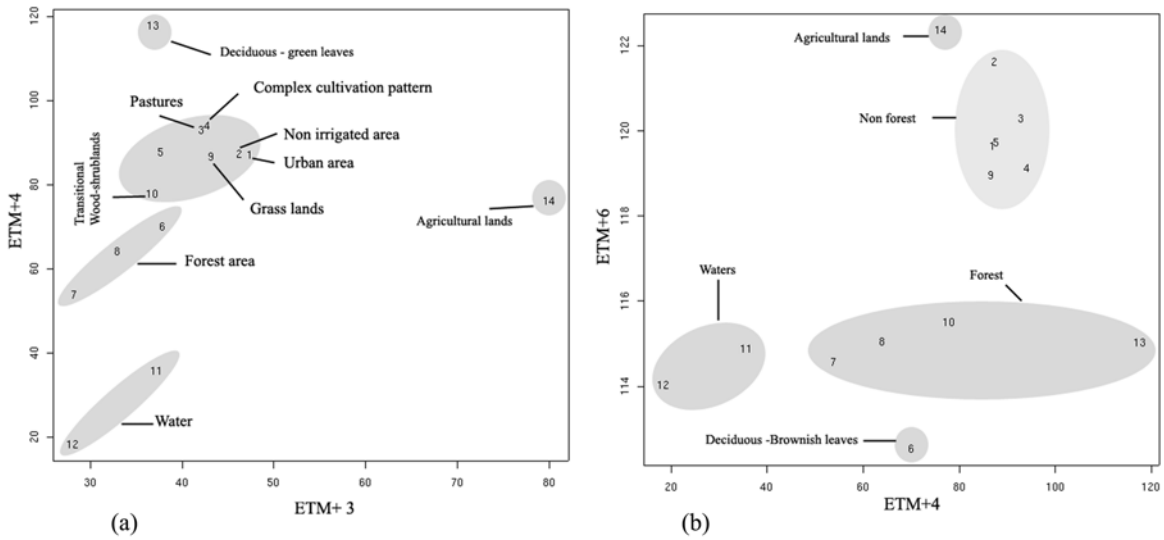

Fig. 3. Distribution of the land covers classes in two-dimensional feature spaces.

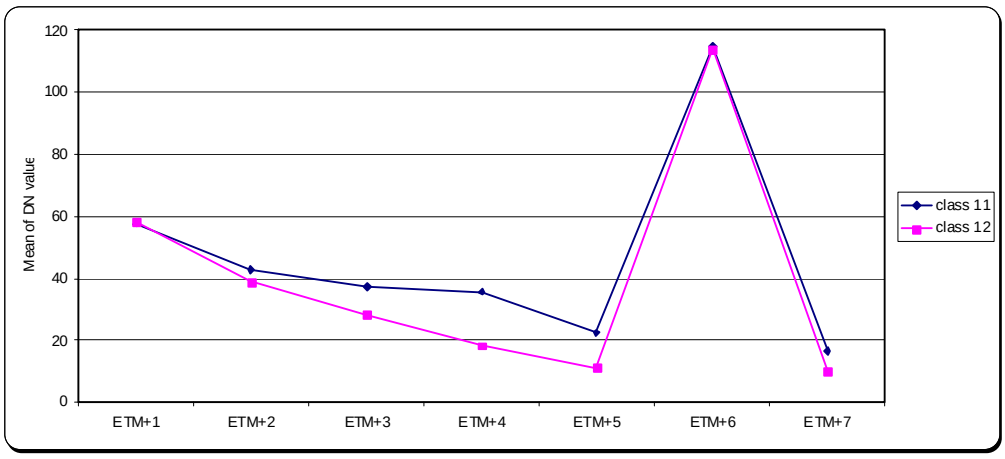

Fig. 4. Spectral signatures of two water classes, class 11 (water courses) and, class 12 (water bodies).

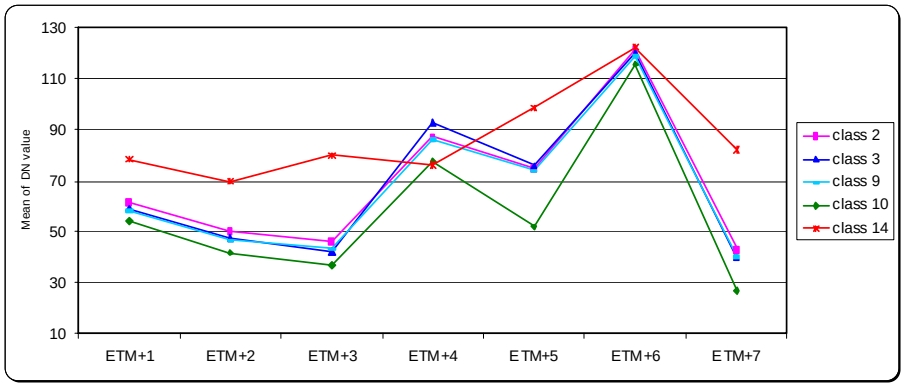

Fig. 1. Spectral signatures of Forest land covers (Class description in table 1).

Table. 1. Description of Land cover classes of the study area.

Class NO	Classes	Description
1	Discontinuous Urban Fabric	Buildings, roads, villages, structures, small gardens and orchards.
2	Non-irrigated arable lands	Includes cereals, open fields, vegetables.
3	Pastures	Dense grass covers and graminaceas mainly use for grazing.
4	Complex cultivation patterns	includes parcels of permanent crops, pasture and/or permanent crops.
5	Land occupied by agriculture with significant area of natural vegetation	Areas principally occupied by agriculture, interspersed with significant natural areas.
6	Broad leaved forest with brown leaves	Deciduous forest represents more than 75% of class-with brownish leaves color on September.
7	Coniferous	Coniferous forest represents more than 75% of class.
8	Mixed forest	Neither broad-lived nor coniferous species predominate.
9	Natural grass lands	Often situated in areas of rough, uneven ground. At least 75 % of the surface covered by natural vegetation.
10	Transitional woodland-shrub	Include bushy vegetation with scattered trees.
11	water courses	Include rivers and canals.
12	water bodies	Lake includes reservoirs.
13	Broad leaved with green leaves	Deciduous forest represents more than 75% of class-with greenish leaves color on September.
14	Agricultural lands	Land mostly used for agriculture.

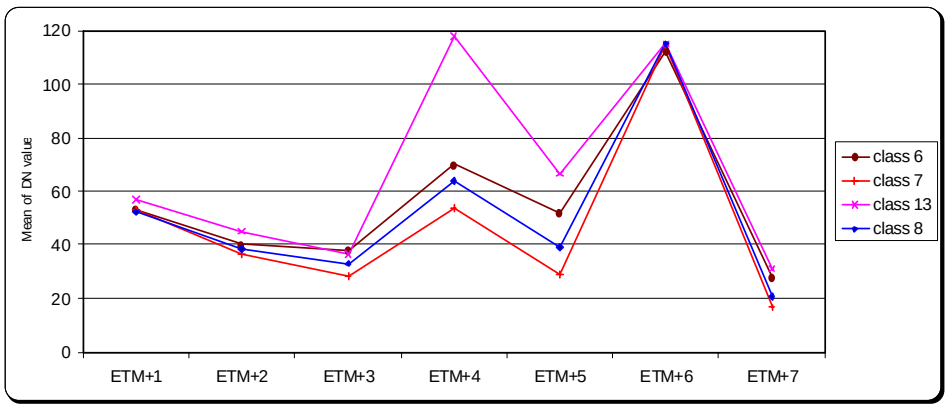

Fig. 6. Spectral signatures of non-forest land cover (Classes descriptions are in table 1).

After feature space and spectral signatures analysis, the data are classified using nine band combinations and the two described methods. In overall 18 classified images are achieved and accuracies examined. Figure 7 shows four result produced with the Sequential Maximum a Posteriori (SMAP) method. The result shows that SMAP as the superior method can improve Kappa values for all band combinations with on average 17% compared to ML algorithm (figure 8). This is due to the nature of the SMAP algorithms that consider the texture and spatial information. This result confirm the finding of other researchers (Bouman and Shapiro, 1994; McCauley and Engel, 1977; Zhou & Robson, 2001). The result maps showed that the dominant land cover of the Carpathian ridge is the deciduous forest. The discontinuous urban fabrics (class no.1) are the major land covers on the lower part of the southwestern (Slovakian side), south and northeastern (Ukrainian side) of the study area. The lower areas in the southwestern regions are dominated by agricultural lands (class no.14).

The highest Kappa accuracy of 80.37 % and 64.36 % is achieved respectively using all 7 bands for both SMAP and ML classifications algorithm. Excluding the thermal band from classification (classification with 6 reflective bands) decreased the Kappa values by about 8% for both algorithms. The band combination including PC1, 2, 3, and 4 (PCA calculated for all 7 bands) produced the same Kappa value as bands 3, 4, 5 and 6.

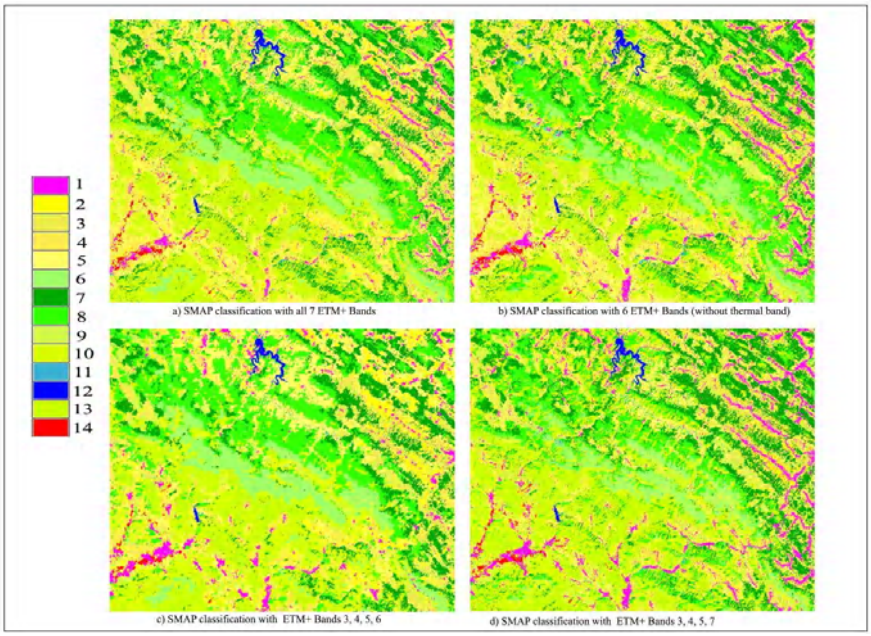

Fig. 7.Classification results with Sequential Maximum a Posteriori (SMAP) method (Class descriptions refer to table 1).

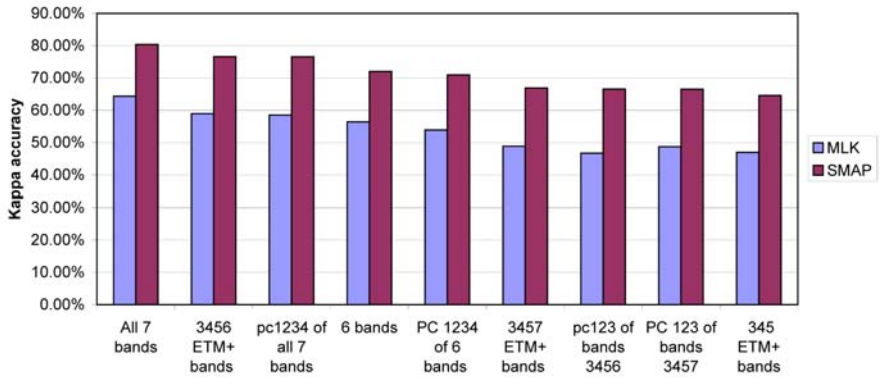

Fig. 8. Kappa accuracies of the classification results with two Sequential Maximum a Posteriori (SMAP) and traditional per-pixel Maximum likelihood (ML) algorithms.

The Kappa value for band combination 3, 4, 5 and 6 (The first and second ranks of OIF with inclusion of thermal band) was also about 4% higher than using 6 bands without the thermal band for both algorithms. Lowest kappa accuracy for both classification methods is achieved with 3, 4 and 5 ETM+ bands (ML=46% and SMAP= 64%). Details of class accuracy with contribution of all bands in SMAP algorithm for each land cover classes are also provided to explore the role of the reflective and thermal bands in accuracy improvement (Figure 9). Using all 7 ETM+ bands in SMAP algorithms improved the accuracy of land cover classes 2, 3, 4, 5, 6, 8, 9 and 10. The already high accuracy for five classes including waters (class no 11 and 12), agricultural lands (class no.14), coniferous forest (class no. 7) and deciduous with green leaves did not increase with thermal band and remained at the same levels. The size, shape and thermal properties of various land cover classes play an important role in differentiating between them. Some features are warming up more quickly than other classes and in some cases may have the same effective blackbody temperatures. So in these cases, there is not a good thermal differentiation and inclusion of thermal band may not help to improve accuracy. Coupled with the fact that some of the classes were small (agricultural lands or discontinuous urban fabrics) in comparison with the conflicting classes (various pastures, grasslands or residential pattern), sufficient thermal differences may not exist. Following the inclusion of the thermal data, the kappa accuracy is greatly increased for the classes no.2 (non-irrigated arable lands) and no. 4 (complex cultivation lands). Class no.1 (discontinuous urban fabric) which includes the buildings, roads, villages, structures, small gardens and orchards due to high variability in feature, close thermal radiation properties and possibly small diurnal changes, is the only land cover class which inclusion thermal band in classification reduces its Kappa accuracy's about 21%. Examination of other band combinations based on the optimum index factor (OIF) calculation produced the same results and confirmed these finding (Figure 10). The Kappa statistics and measures of variances derived from the confusion matrices were examined to determine if the results of the classification methods are statistically different from one another at a 95% confidence interval (Table 2). All the possible pairing of the classification methods were tested and result of Z scores showed that all pairs of the two classification methods are different at 95% confidence level (Z-Score >1.96).

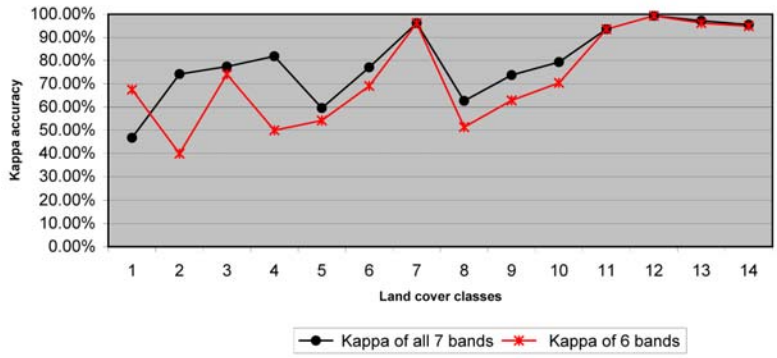

Fig. 9. Kappa accuracies of the land cover classes with Sequential Maximum a Posteriori (SMAP) algorithm with and without thermal bands inclusion in the data set (Class description in table 1).

Table 2. Z test of classification results to determine significant differences among the classification results.

Band Combinations	ML	SMAP	VAR MLK	VAR SMAP	Z-Score (95%)
All 7 bands	0.64	0.80	0.000026	0.000018	24.12
3456 ETM+ bands	0.59	0.77	0.000028	0.000021	25.19
pc1234 of all 7 bands	0.59	0.77	0.000028	0.000021	25.77
6 bands	0.56	0.72	0.000029	0.000023	21.66
PC 1234 of 6 bands	0.54	0.71	0.000278	0.000023	9.84
3457 ETM+ bands	0.49	0.67	0.00003	0.000025	24.35
PC123 of bands 3456	0.47	0.67	0.000029	0.000025	27.04
PC 123 of bands 3457	0.49	0.67	0.00028	0.000025	10.21
345 ETM+ bands	0.47	0.65	0.000029	0.000026	23.73

ML= Maximum likelihood, SMAP = Sequential Maximum a Posteriori, VAR = variance.

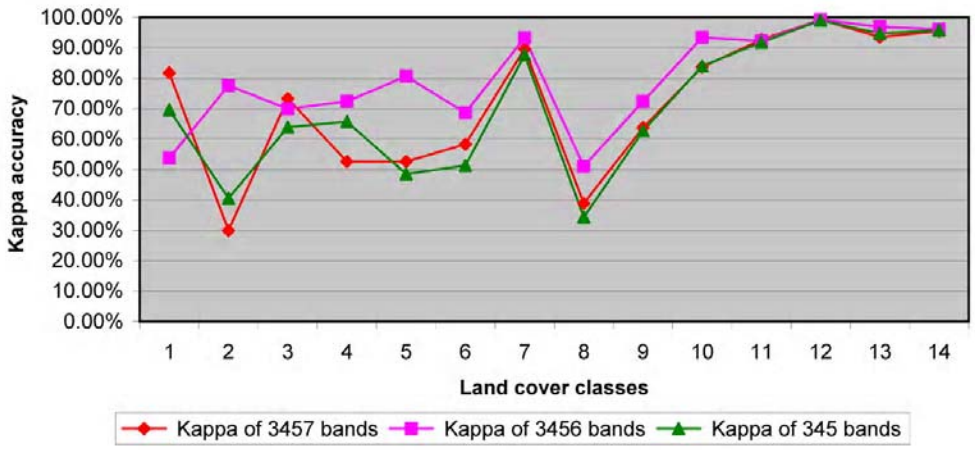

Fig. 10. Kappa accuracies of the land cover classes with Sequential Maximum a Posteriori (SMAP) algorithm with and without inclusion of the thermal band in the data set. These band combinations are selected based on the OIF calculation with and without thermal bands inclusion. (Class description in table 1).

CONCLUSION

The major obstacle for using remote sensing data for land cover classification is the similarity some of the surface spectral characteristics under a wide range of environmental conditions. Combining thermal and reflective information can help to differentiate between similar classes. Thermal band due to lower spatial resolution (60 meter in Landsat 7) compared with reflective bands (30 meter) are excluded from classification processing in most studies. In this study we showed that the thermal band coupled with proper classification algorithms like Sequential Maximum a Posteriori (SMAP) algorithm could significantly increase the kappa accuracy for most of land cover classes. This indicates that the thermal data can aid in classifying certain land cover classes providing that there is a good thermal differentiation properties. Using first and second ranks of the optimum index factor (OIF) calculation with inclusion of thermal band in data set may provide the best bands combination for classifications. Supplying thermal band in band combination in order to combine emitted and reflective information is necessary and may enhance the accuracy. But some features are warming up more quickly than other classes and in some cases may reach the same effective blackbody temperatures. Thus in these cases, due to close radiation temperature, inclusion of thermal band may not help to improve accuracy. Coupled with small size of some of the classes (agricultural lands or discontinues urban fabrics) in comparison with the conflicting classes (various pastures, grasslands or residential pattern), sufficient thermal differences may not exist.

ACKNOWLEDGEMENT

We are grateful to Swedish Institute for funding all travel expenses in the framework of the Visby program. We like to thank the University of Tehran, International Desert Research Center and all our colleagues especially Docent Ivan Kruhlov, Department of Physical Geography, Ivan Franko University in Lvov, Ukraine and Dr. Mieczyslaw Sobik, Institute of Geography and Regional Development, University Wroclaw, Poland for interesting discussions and for providing facilities and support.

REFERENCES

Alavi Panah, S. K., Komaki, C. B., Goorabi, A. and Matinfar, H. R. (2007). Characterizing Land Cover Types and Surface Condition of Yardang Region in Lut Desert (Iran) Based upon Landsat Satellite Images. World Applied Sciences Journal, **2 (3)**, 212-228.

Alesheikh, A. A., Ghorbanali, A. and Nouri, N. (2007). Coastline change detection using remote sensing. Int. J. Environ. Sci. Tech., **4 (1)**, 61-66.

Borak, J. S. and Strahler, A. H. (1999). Feature selection and land cover classification of a MODIS-like data set for a semiarid environment. International Journal of Remote Sensing, **20**, 919-938.

Bouman, C.A. and Shapiro, M. (1994). A Multiscale Random Field Model for Bayesian Image Segmentation. IEEE Transaction on Image Processing, **3 (2)**, 162-177.

Cetin, M. (2009). A satellite based assessment of the impact of urban expansion around a lagoon. Int. J. Environ. Sci. Tech., **6 (4)**, 579-590.

Chavez, P. S., Guptill, S. C. and Bowell, J. A. (1984). Statistical method for selecting landsat MSS Ratios. Journal of Applied Photographic Engineering, 8, 23-30.

Chintan, A. S., Arora, M. K., and Pramod, K. V. (2004). Unsupervised classification of hyperspectral data: an ICA mixture model based approach International Journal of Remote Sensing, **25**, 481-487.

Cihlar, J. (2001). Land cover mapping of large areas from satellites: status and research priorities. International Journal of Remote Sensing, **21 (6,7)**, 1093-1114.

Congalton, R. G., and Green, K. (1999). Assessing the accuracy of remotely sensed data: principles and practices. New York: Lewis publishers.

Dale, A.Q., and Jeffrey , C. L. (1999). Thermal infrared remote sensing for analysis of landscape ecological processes: methods and applications. Landscape Ecology., **14 (6)**, 577-598.

Dator, J., Goossens, R., and Van Ranst, E. (1998). The use of remote sensing to map gypsiferous soils in the Ismailia Province (Egypt). Geoderma, **87 (1)**, 47-56.

Dean, A. M., and Smith, G. M. (2003). An evaluation of per-parcel land cover mapping using maximum likelihood class probabilities. International Journal of Remote Sensing, **24**, 2905-2920.

Gao, Y., Mas, J. F., Maathuis, B. H. P., Xiangmin, Z., and Dijk, P. M. V. (2006). Comparison of pixel-based and object-oriented image classification approaches—a case study in a coal fire area, Wuda, Inner Mongolia, China. International Journal of Remote Sensing, **27 (18)**, 4039-4055.

GRASS Development Team. (2006). Geographic Resources Analysis Support System (GRASS), GNU General Public License. Eletronic document. http://grass.itc.it.

Kuemmerle, T., Volker, C. R., Perzanowski, K., and Hostert, P. (2006). Cross-border comparison of land cover and landscape pattern in Eastern Europe using a hybrid classification technique. Remote Sensing of Environment, **103**, 449-464.

McCauley, J. F., Grolier, M. J., and Breed, C. S. (1977). Yardangs. In D.O. Doehring (Ed.), Geomorphology in Arid Regions (pp. 233-269). London: Allen and Unwin.

Miliaresis, G. C., and Paraschou, C. V. E. (2005). Vertical accuracy of the SRTM DTED level 1 of Crete. International Journal of Applied Earth Observation and Geoinformation, **7**, 49-59.

Ouattara, T., Gwyn, Q. H. J., and Dubois, J. M. M. (2004). Evaluation of the runoff potential in high relief semi-arid regions using remote sensing data: application to Bolivia. International Journal of Remote Sensing, **25**, 423-435.

Pijanowski, B.C., Tayyebi, A., Delavar, M. R. and Yazdanpanah, M. J. (2009). Urban Expansion Simulation Using Geospatial Information System and Artificial Neural Networks. Int. Journal. Environ. Res., **3 (4)**, 493-502.

Pizzolato, A. N., and Haertel, V. (2003). On the application of Gabor filtering in supervised image classification. International Journal of Remote Sensing, **24**, 2167-2189.

Shobeiri, S. M. , Omidvar, B. and Prahallada, N. N. (2007). Digital Change Detection Using Remotely Sensed Data for Monitoring Green Space Destruction in Tabriz. Int. J. Environ. Res., **1 (1)**, 35-41.

Solaimani, K. and Modallaldoust, S. and Lotfi, S. (2009). Investigation of land use changes on soil erosion process using geographical information system. Int. J. Environ. Sci. Tech., **6 (3)**, 415-424.

Zhou, Q., and Robson, M. (2001). Contextual information is ultimately necessary if one is to obtain accurate image classifications. . International Journal of Remote Sensing, **22**, 3457-3470.